Clays and Clay Minerals, Vol. 57, No. 1, 46–53, 2009.

MAGNETIC ENHANCEMENT DURING THE CRYSTALLIZATION OF FERRIHYDRITE AT 25 AND 50ºC

E. Cabello[1], M. P. Morales[2], C. J. Serna[2], V. Barrón[1,*], and J. Torrent[1]

[1] Departamento de Ciencias y Recursos Agrícolas y Forestales, Universidad de Córdoba, Edificio C4, Campus de Rabanales, 14071 Córdoba, Spain

[2] Instituto de Ciencia de Materiales de Madrid, CSIC, Sor Juana Inés de la Cruz 3, 28049 Madrid, Spain

Abstract—Soil formation usually results in an increase in magnetic susceptibility. The magnetic properties of the products of transformation of ferrihydrite, a typical precursor of other soil Fe oxides, were examined in the present work. Synthetic 2-line ferrihydrite was aged at two temperatures (25 and 50ºC) and two different relative humidities (80 and 100%) in the presence of silicate, phosphate, citrate, and tartrate as adsorbed ligands (molar anion/Fe ratio = 1–3%). The ligands delayed or prevented the transformation of ferrihydrite to hematite. The magnetic susceptibility of the ferrihydrite transformation products increased with aging, the rate of increase depending on the type of ligand added and its concentration. The largest increase in magnetic susceptibility, sixfold, was obtained with ferrihydrite in a citrate/Fe ratio of 1%, after 1500 days. The resulting magnetic products exihibited superparamagnetic behavior at room temperature and high coercivity at 5 K. The formation of an intermediate ferrimagnetic phase in the ferrihydrite-to-hematite transformation might explain the magnetic enhancement observed in many aerobic soils lacking other sources of magnetic minerals.

Key Words—Crystallization, Ferrihydrite, Ferrimagnetism, Hematite, Maghemite.

INTRODUCTION

The formation of Fe oxides (a term used here to describe oxides, hydroxides, and oxyhydroxides of Fe) in soils and sediments is governed by environmental factors such as temperature, moisture content, aeration, pH, and the concentrations of various ions in solution (Cornell and Schwertmann, 2003, and references therein). Generally, the first product of the weathering of primary Fe-bearing minerals is ferrihydrite, a low-crystallinity Fe oxyhydroxide ($Fe_5HO_8{\cdot}4H_2O$). This mineral can be further transformed *via* different pathways to the more common crystalline Fe oxides – goethite (α-FeOOH) and hematite (α-Fe_2O_3), mainly. The transformation of ferrihydrite to hematite occurs *via* a mechanism involving dehydration and rearrangement favored by high temperature, low water activity, and near-neutral pH values (Torrent and Guzmán, 1982; Torrent *et al*., 1982; Schwertmann, 1985; Gálvez *et al*., 1999). Foreign ions can be adsorbed onto the ferrihydrite surface and affect its rate of transformation and the nature of the end products (*e.g.* their hematite/goethite ratio) (Cornell and Schwertmann, 2003). Barrón and Torrent (2002), Barrón *et al*. (2003), and Liu *et al*. (2008) showed that the presence of adsorbed phosphate and citrate delayed the hydrothermal (T>100ºC) transformation of ferrihydrite to hematite and produced an intermediate magnetic phase which was designated 'hydromaghemite' on account of its similarity to maghemite (γ-Fe_2O_3): the X-ray diffraction (XRD) pattern and Mössbauer spectrum for such a phase are consistent with the presence of an intimate mixture of 6-line ferrihydrite and defective maghemite, even though the transmission electron microscopy (TEM) images only show optically homogeneous particles spanning a narrow size-distribution range (10–25 nm).

The origin of the unbalanced magnetic moment in hydromaghemite remains obscure. Recent synchrotron-based X-ray total scattering observations suggest that synthetic ferrihydrites with average domain sizes of 2, 3, and 6 nm differ little in terms of the underlying structure; the differences in their diffraction patterns have been ascribed to changes in average size in the coherent scattering domains (Michel *et al*., 2007b). Michel *et al*. (2007a) also proposed a new structure for ferrihydrite containing 20% of tetrahedrally and 80% of octahedrally coordinated Fe. This structure leads to an unbalanced magnetic moment and can thus result in significant ferrimagnetism, especially in the best-ordered ferrihydrite types (*i.e.* those with more than three XRD lines). In this context, hydromaghemite could be the final step in the progressive crystallization, increase in crystal size, and build-up of a net magnetic moment preceding the transformation to hematite. As previously reported for the transformation of stoichiometric maghemite to hematite (Chernyshova *et al*., 2007; Bomatí-Miguel *et al*., 2008; Navrotsky *et al*., 2008) and γ-Al_2O_3 to α-Al_2O_3 (McHale *et al*., 1997), such a transformation is likely to depend on particle size; surface-enthalpy calculations indicate that the γ phase

* E-mail address of corresponding author:
cr1balov@uco.es
DOI: 10.1346/CCMN.2009.0570105

becomes unstable relative to the α phase at smaller than a certain surface area (*i.e.* greater than a certain particle size).

The evolution of 2-line ferrihydrite at temperatures and water activities typical of Earth-surface environments are shown here to involve a progressive increase in magnetic susceptibility before eventual transformation to hematite. The potential significance of the magnetic enhancement in soils lacking other sources of magnetic minerals is also discussed.

MATERIALS AND METHODS

Various 2-line ferrihydrites were prepared by neutralizing 0.1 M $Fe(NO_3)_3$ with 5% NH_4OH to a final pH of 7 in the presence of either silicate, phosphate, tartrate, or citrate at an initial anion/Fe mole ratio of 0, 1, 2, or 3%. No greater ratios were used as they are unlikely to occur in natural environments and have been found to prevent the transformation of ferrihydrite (Cornell and Schwertmann, 2003). The ferrihydrite precipitates obtained were washed with deionized water by repeatedly centrifuging the suspension and decanting the supernatant until the electrical conductivity of the equilibrium solution was <10 μS cm^{-1}. Then they were freeze-dried and ground to a fine powder. For the ferrihydrite transformation experiments, ~1 g of the powder was spread onto the bottom of a cylindrical polystyrene container, 2.5 cm in diameter, which was placed in a humidity chamber. The transformation was studied at two temperatures (25 and 50ºC), two water activities (0.8 and 1), and in the presence of four anions (silicate, phosphate, citrate, and tartrate) at the anion/Fe ratios stated above. Saturated solutions of KCl (at 25ºC) or KNO_3 (at 50ºC) were placed at the bottom of the humidity chamber to maintain the water activity at 0.8 (*i.e.* 80% relative humidity, RH), and pure water was used to keep water activity at 1.0 (*i.e.* 100% RH).

Powder XRD patterns were obtained using a Siemens D5000 diffractometer equipped with CoKα radiation and a graphite monochromator, using a step size of 0.05º2θ and a counting time of 10 s. For TEM, the products were prepared by depositing a drop of dilute aqueous suspension on a C-coated grid for examination using a JEOL JEM-2010 instrument. The specific surface area (BET method; Brunauer *et al*., 1938) and micropore surface area (*t*-plot method; Lippens and de Boer, 1965) were determined by N_2 adsorption, using a Micromeritics ASAP 2010 surface area analyzer. Color was determined using a Varian Cary 5000 spectrophotometer equipped with a diffuse reflectance attachment. Reflectance values were taken at 0.5 nm intervals over the 380–710 nm range and converted to Munsell color parameters as reported by Barrón and Torrent (1986).

Low-field magnetic susceptibility, χ, was measured using a Bartington MS 2B dual-frequency sensor (Bartington Instruments Ltd., Oxford, UK) at a low frequency (0.47 kHz). Maximum magnetization (M_{max}) and coercivity (H_c) were calculated from the magnetization curves after applying a sufficient magnetic field to saturate the samples, *i.e.* 3 T at room temperature and 5 T at 5 K, using a vibrating sample magnetometer (MLVM9MAGLAB 9T, Oxford Instruments). Samples were prepared by packing the powder into a plastic tube such that the axial ratio of the resulting sample was >5. In this way, the need to correct for sample-shape demagnetizing effects was avoided. In addition, the variation of magnetization as a function of the temperature under heating in a constant field of 10 mT was recorded, either after zero-field cooling (ZFC) or after cooling in a field of 10 mT (FC). The ZFC/FC curves provide information about the blocking temperature (T_B) below which magnetization is stable against thermal agitation, hysteresis occurs, and superparamagnetism disappears. For a particle of volume, V, and uniaxial anisotropy, the blocking temperature depends on the anisotropy and particle volume as follows (Cullity, 1972):

$$T_B k_B = K_{eff} V \ln (\tau_m/\tau_0) \quad (1)$$

where k_B is the Boltzmann constant; K_{eff}, the anisotropy constant; τ_m, the measuring time; and $\tau_0 = 10^{-9}$–10^{-11} s, according to the Néel-Brown model (Coffey *et al*., 1993). Therefore, for vibrating sample magnetometer measurements, $T_B = K_{eff} V/25\ k_B$

RESULTS

Transformation of pure ferrihydrite

Pure ferrihydrite was gradually transformed to hematite on aging at 50ºC at 100% RH. As can be seen from the XRD patterns for the 0–90 day aging period (Figure 1), the two broad peaks typical of 2-line ferrihydrite were gradually replaced by the sharp peaks typical of highly crystalline hematite, consistent with the results of similar previous experiments (*e.g.* Torrent *et al*., 1982). Under the TEM, the aged ferrihydrite at 50ºC and 100% RH for 25 days (Figure 2b) looked very similar to the fresh ferrihydrite (Figure 2a) and exhibited aggregates of subspherical particles 4–6 nm in size. However, the hematite formed after 90 days exhibited rounded particles of 25–50 nm (Figure 2c). The specific surface area of the initial ferrihydrite was 297 $m^2\ g^{-1}$ (98% in micropores), and that of hematite, 72 $m^2\ g^{-1}$ (with a negligible proportion of micropores). The color (Munsell notation) was 3.96 YR 2.9/2.9 for the initial ferrihydrite and 8.7R 3.4/4.1 for the resulting hematite. By contrast, no changes in XRD pattern, particle morphology, color, or specific surface area were observed in pure ferrihydrite aged at 25ºC for 1200 days.

The increase in χ for pure ferrihydrite aged at 100% RH (Figure 3) was sustained, but modest, at 25ºC (from 1.2×10^{-6} $m^3\ kg^{-1}$ at day 0 to 2.2×10^{-6} $m^3\ kg^{-1}$ at day 1500). By contrast, the initial rate of increase in χ was

https://doi.org/10.1346/CCMN.2009.0570105 Published online by Cambridge University Press

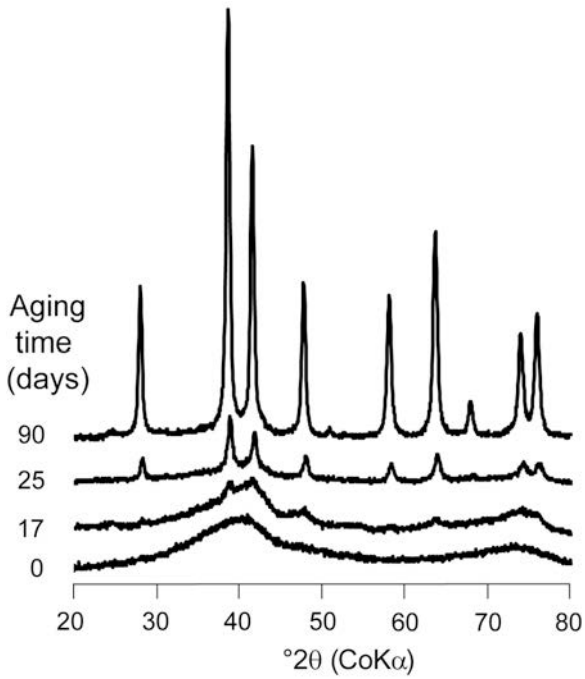

Figure 1. XRD patterns for the succesive products obtained by aging pure ferrihydrite at 50ºC at 100% RH for 90 days.

much greater at 50ºC; thus, χ was 2.4×10^{-6} m^3 kg^{-1} at day 50. Then, χ dropped sharply to ~0.5×10^{-6} m^3 kg^{-1} at day 90 when, based on the XRD pattern, conversion to hematite was essentially complete. In summary, the effect of increasing the temperature was an accelerated magnetic enhancement and the transformation of the intermediate phase to hematite.

The experiments conducted at 80% RH provided similar results (not shown), the difference being that the rates of change of χ and transformation of ferrihydrite to hematite were slightly smaller at 80% than at 100% RH. This was also the case with adsorbates described below. For this reason, only the results of the experiments performed at 100% RH are discussed in the following sections.

Transformation of ferrihydrite in the presence of foreign anions

As with pure ferrihydrite, increasing the temperature accelerated the magnetic enhancement and the eventual transformation of the anion-doped ferrihydrites to hematite. For this reason, only the results obtained at 50ºC are shown (Figure 4).

Increasing the anion/Fe ratio from 1 to 3% decreased the rate of increase of χ with all anions (*i.e.* the adsorbed anions delayed magnetic enhancement in the intermediate phase). The adsorbed anions also retarded or prevented further transformation of this phase to hematite (as suggested by a sharp drop of χ to a value of ~0.5×10^{-6} m^3 kg^{-1}). Therefore, no hematite was

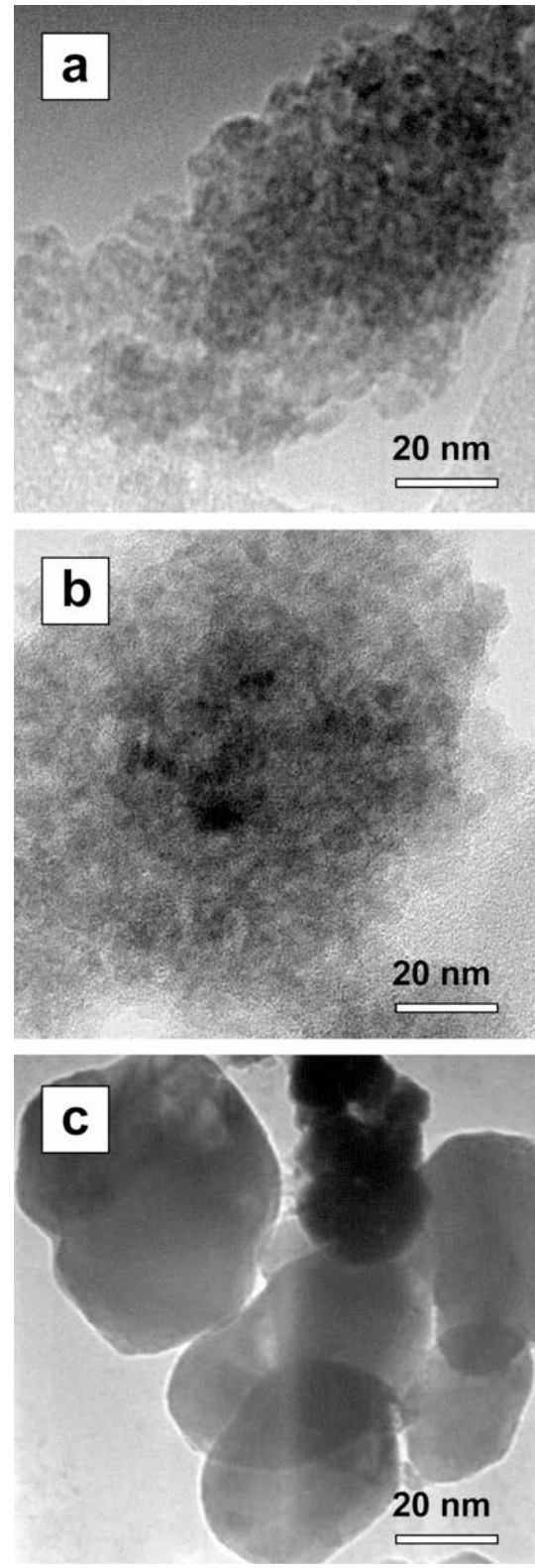

Figure 2. TEM images of (a) fresh ferrihydrite, (b) the product obtained by aging at 50ºC and 100% RH for 25 days, and (c) hematite formed at 50ºC at 100% RH after 90 days.

https://doi.org/10.1346/CCMN.2009.0570105 Published online by Cambridge University Press

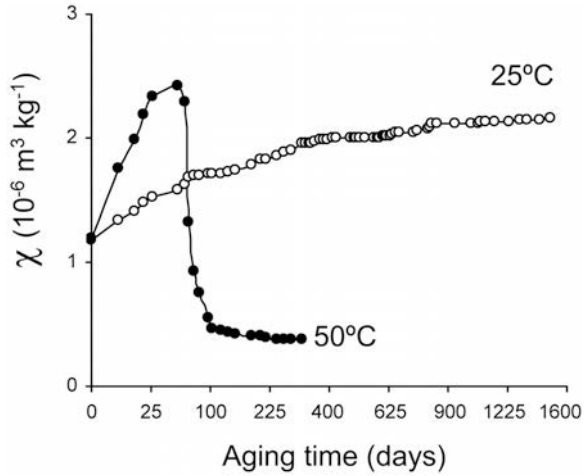

Figure 3. Magnetic susceptibility as a function of aging time for the products formed from pure ferrihydrite at 25 and 50ºC, at 100% RH.

formed at phosphate/Fe ratios of 2 and 3% or at any citrate/Fe ratio. Both the capacity of the different anions to hinder crystallization and the maximum value of χ increased in the following sequence: silicate < tartrate < phosphate < citrate. This sequence coincides with that of affinity of the anions for the Fe oxide surfaces (Cornell and Schwertmann, 1979; Reeves and Mann, 1991; Glasauer *et al.*, 1999; Gálvez *et al.*, 1999).

In contrast to the aforementioned hydromaghemite-rich samples prepared from anion-doped 2-line ferrihydrite at >100ºC (Barrón and Torrent, 2002; Barrón *et al.*, 2003, Liu *et al.*, 2008), using XRD, TEM, or Mössbauer spectroscopy to identify and characterize the intermediate phase responsible for the several-fold magnetic susceptibility enhancement observed in some samples was not possible. According to the Arrhenius law, an extrapolation of the results from high- to room-temperatures should lead to aging times of several thousand years to obtain the same product. Nevertheles, the hysteresis loops and the ZRC/FC curves provided more magnetic information about the properties of this intermediate phase.

Superparamagnetic behavior was observed at room temperature in all the intermediates, whether or not an

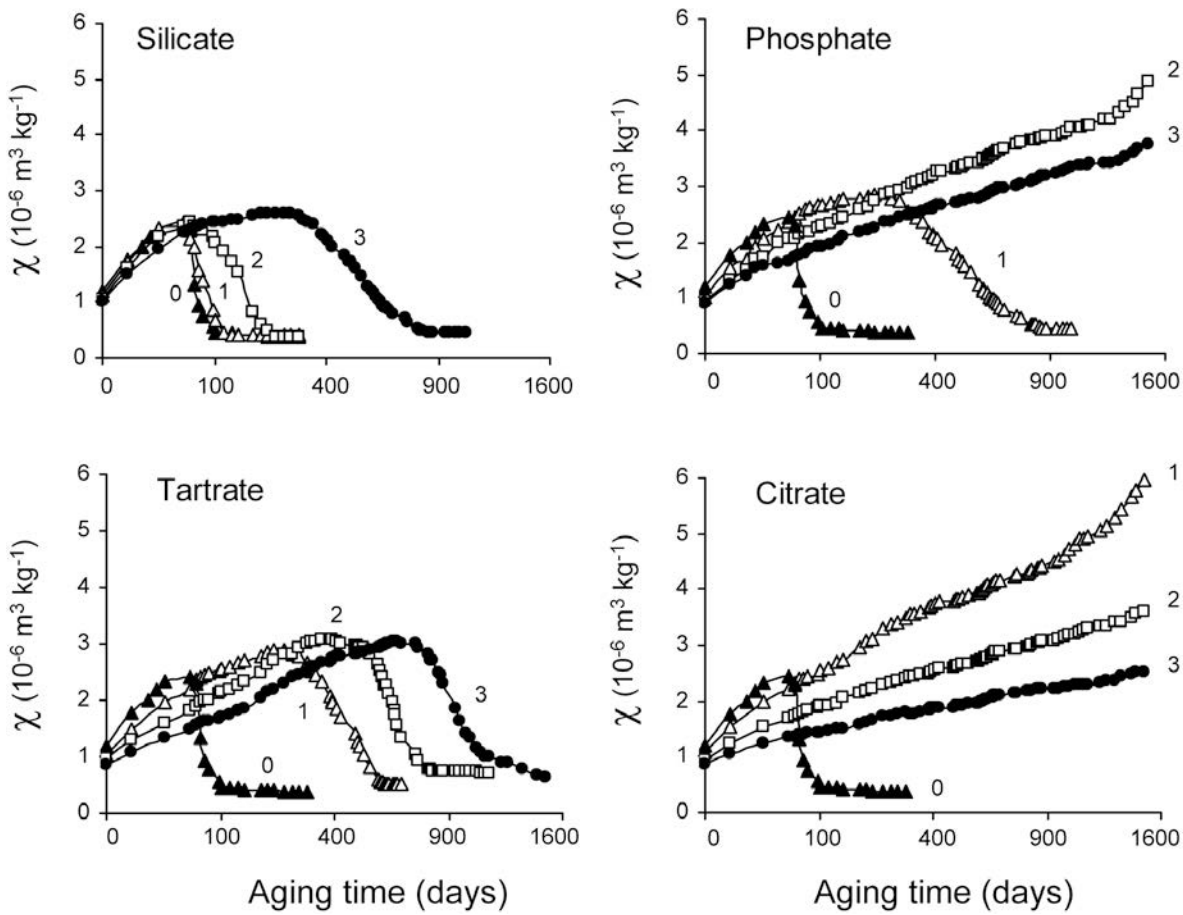

Figure 4. Magnetic susceptibility as a function of aging time (at 50ºC at 100% RH) for the products formed from ferrihydrite prepared in the presence of silicate, tartrate, phosphate, or citrate, at an anion/Fe mole ratio of 0, 1, 2, or 3%.

https://doi.org/10.1346/CCMN.2009.0570105 Published online by Cambridge University Press

additive was used (Figure 5). However, for the 1% citrate ferrihydrite, the Langevin curvature started to become visible at lower H values, suggesting an increased spin order. At 5 K, the intermediate samples exhibited ferromagnetic behavior, with hysteresis loops and an extremely large coercivity (200 mT; Figure 5) which is typical of magnetic particles such as ferrihydrite (Duarte *et al*., 2006) or maghemite smaller than a certain critical size with an extra source of anisotropy apart from the crystalline one (Morales *et al*., 1999). Maximum magnetization (M_{max}) was increased by the presence of additives, where it followed the same trend as at room temperature. The greatest M_{max} value, 15.5 A m^2kg^{-1}, was that for the sample treated with 1% citrate and the lowest, 12 A m^2 kg^{-1}, that for pure ferrihydrite. Increased M_{max} values can be associated with the greater spin-order structures of the coarser particles or to surfaces containing a smaller proportion of defects. Indeed, the magnetic behavior of an assembly of magnetic nanoparticles, with a volume distribution and randomly oriented easy axis, poses a complex problem due to the coexistence of finite size and surface effects in addition to the presence of magnetic interparticle interactions (Battle and Labarta, 2002).

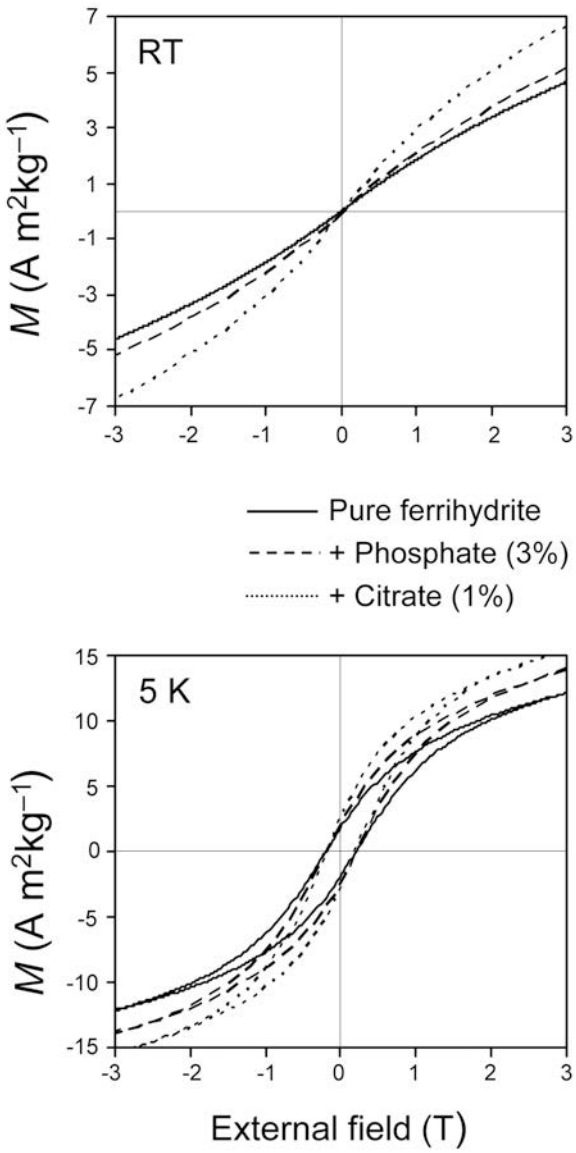

Figure 5. Magnetization curves (magnetic moment M vs. external magnetic field (Tesla)) obtained at room temperature and 5 K for pure ferrihydrite aged for 50 days and ferrihydrites prepared in the presence of phosphate (anion/Fe mole ratio of 3%) or citrate (anion/Fe mole ratio of 1%) aged at 50ºC at 100% RH for 1100 days.

The ZFC/FC measurements for the ferrihydrite treated with 1% citrate in the initial state and after 1100 days of aging (Figure 6) showed that the samples were superparamagnetic at room temperature and become blocked below the blocking temperature (T_B), which is 57 K for the initial ferrihydrite and 61 K for the aged ferrihydrite. Note that T_B is related to anisotropy and particle size in such a way that low T_B values correspond to low anisotropy or small particle sizes (equation 1). The shape of the ZFC/FC curves is consistent with a narrow particle-size distribution for both samples. Some aggregation may also occur, as suggested by the differences between the ZFC and the FC curves above T_B.

DISCUSSION

Aggregation, dehydration, and transformation of ferrihydrite to hematite are quick in the presence of few or no adsorbates. As a result, the formation of a well crystallized ferrihydrite intermediate is imperceptible. By contrast, when adsorbed ligands are present in significant amounts, the pristine ferrimagnetic behavior

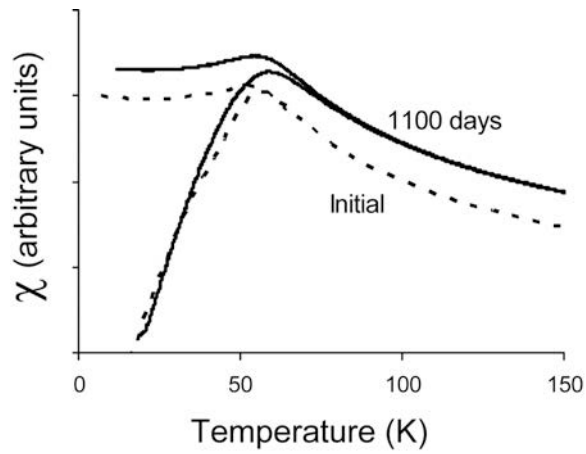

Figure 6. Temperature dependence of the magnetic susceptibility under field-cooled (FC) at 10 mT and zero-field-cooled (ZFC) conditions for the initial ferrihydrite prepared in the presence of citrate (anion/Fe mole ratio of 1%) and aged at 50ºC at 100% RH for 1100 days.

https://doi.org/10.1346/CCMN.2009.0570105 Published online by Cambridge University Press

of successive intermediates in the slow ferrihydrite-to-hematite transformation is quite apparent. Such ferrimagnetic behavior may be related to subtle changes in the structure of ferrihydrite; this is a subject of some debate (Jambor and Dutrizac, 1998). By using extended X-ray absorption fine structure (EXAFS) and Fe X-ray absorption near edge structure (XANES) (Manceau and Gates, 1997; Wilke *et al*., 2001), and neutron diffraction (Jansen *et al*., 2002), no tetrahedral Fe was detected in ferrihydrite. By contrast, Eggleton and Fitzpatrick (1988) using XRD, Zhao *et al*. (1994) using EXAFS and XANES, and Janney *et al*. (2000, 2001) using nanodiffraction measurements found that Fe can occur in both tetrahedral and octahedral coordination in ferrihydrite. Michel *et al*. (2007a) performed total elastic X-ray scattering experiments on 2-, 3-, and 6-line ferrihydrites and proposed a new structure model based on pair-distribution function calculations. This structural model incorporates 20% of tetrahedrally and 80% of octahedrally coordinated Fe in an arrangement that might result in ferrimagnetic behavior. The calculated XRD patterns for this structure are similar to the experimental XRD patterns with 10 broad lines obtained in ferrihydrite hydrothermal transformation experiments (Barrón *et al*. 2003). However, in the present room-temperature experiments, only two broad lines were observed in the XRD pattern, even for the intermediates exhibiting the greatest magnetic susceptibility.

The opportunities for crystal growth and reordering of ferrihydrite (and concomitant magnetic enhancement) before transformation to hematite are limited. In this respect, the relative stability of the γ- and α-$Fe(Al)_2O_3$ phases (McHale *et al*., 1997; Chernyshova *et al*., 2007; Bomatí-Miguel *et al*., 2008; Navrotsky *et al*., 2008) is size dependent, so a crossover surface enthalpy energy for a specific surface area of ~75 $m^2\ g^{-1}$ (~20 nm particle size) determines the phase transformation from the nanosized γ phase (maghemite) to the α phase (hematite) with larger crystals. This could also apply to the ferrihydrite transformation, where increases in crystal size and magnetic susceptibility can be observed only if the presence of adsorbates or the low temperature hinders the formation of hematite.

The magnetic behavior of ferrihydrite has usually been associated with an antiferromagnetic spin arrangement within the core and a small unbalanced magnetic moment arising from defects inside particles and/or from unpaired surface moments (Zergenyi *et al.*, 2000). Based on the aforementioned new structural model (Michel *et al*., 2007a), however, a ferrimagnetic behavior can result from the arrangement of magnetic moments at tetrahedral and octahedral sites, which would be consistent with values of up to 10 Bohr magnetons per unit cell (equivalent to M_s 68 A $m^2\ kg^{-1}$). A similar value was obtained for citrate ferrihydrite aged at 150ºC, which exhibited high crystallinity (Barrón *et al*., 2003). The much lower M_{max} values for the intermediate products studied in this work are consistent with substantially lower crystallinity. The disparate magnetization values obtained suggest a greater spin order for the samples synthesized in the presence of additives. Thus, additives adsorbed onto the surface of the initial particles slowed any transformation process, thereby facilitating the formation of an intermediate phase with a greater spin order structure. Moreover, the presence of adsorbed additives might have reduced spin canting and increased saturation magnetization as a result. Surface-coating effects on the magnitude and uniformity of magnetization in various types of nanoparticles have previously been reported and assigned to quenching of surface moments (Vestal and Zhang, 2003).

The coercivity at low temperature was similar in all samples studied, probably as a result of competition between many different factors including size, surface effects, and magnetic interactions (Battle and Labarta, 2002). An increased spin order inside and at surfaces reduces coercivity; on the other hand, small particle size and interactions between particle scaling with the magnetic moment increase coercivity. Therefore, the presence of additives results in smaller particles of enhanced coercivity. Conversely, the adsorption of additives reduces surface anisotropy (by reducing spin canting), and hence coercivity. These results are consistent with the large anisotropies (up to 50 times greater than those of typical magnetic Fe oxides) of ferrihydrites prepared by different methods (Duarte *et al*., 2006; Silva *et al*., 2006).

The time course of χ suggests that the magnetic behavior of the 1% citrate ferrihydrite is governed by particle size rather than by anisotropy changes. Thus, the slight increase in T_B with time for the aged sample relative to the initial ferrihydrite (Figure 6) indicates a reduction of the energy barrier ($K_{eff}V$), which, as noted before, depends on anisotropy and particle volume. The crystal anisotropy constant is not expected to change with time during the growth process because the crystal structure does not change significantly (judging by the XRD data, Figure 1). Moreover, ferrihydrite particles with different XRD patterns have been shown to possess the same crystal structure irrespective of particle size (Michel *et al*., 2007b). A similar effect of particle size on T_B was previously observed for magnetite nanoparticles coated with oleic acid (Guardia *et al*., 2007).

As proposed by Barrón and Torrent (2002) and Torrent *et al*. (2006), the formation of ferrimagnetic ferrihydrite (a 'hydromaghemite' phase) from the ferrihydrite generated by the weathering of Fe-bearing minerals might be a significant cause of the magnetic enhancement of soil. This hypothesis is plausible for soils in which the parent materials lack magnetite, or in which past fires were not intense enough for other Fe oxides to be thermally transformed to maghemite (Schwertmann, 1985). The presence and concentration of natural organic and inorganic ligands adsorbed on

https://doi.org/10.1346/CCMN.2009.0570105 Published online by Cambridge University Press

ferrihydrite can obviously control the rate of transformation to, and residence time of, this intermediate magnetic phase before its final conversion to hematite. In any case, the crystallization of ferrihydrite in aerobic soils under temperate and warm climates ultimately results in the formation of hematite. For this reason, one can expect the hematite content and magnetic susceptibility (a proxy for the content in the intermediate ferrimagnetic phase) in these soils to be correlated, as is indeed the case (Torrent *et al*., 2006, 2007)

ACKNOWLEDGMENTS

This work was funded by Spain's Ministerio de Educación y Ciencia in the framework of projects AGL2003-01510, AGL2006-10927-CO3-02, MAT2005-03179, and FEDER funds. E. Cabello is grateful to Spain's Ministerio de Educación y Ciencia for a research grant assigned to this project. The authors are also grateful to Dr M.J. Dekkers for his constructive comments and suggestions which greatly improved the quality of this paper.

REFERENCES

Barrón, V. and Torrent, J. (1986) Use of the Kubelka-Munk theory to study the influence of iron-oxides on soil color. *Journal of Soil Science*, **37**, 499–510.

Barrón, V. and Torrent, J. (2002) Evidence for a simple pathway to maghemite in Earth and Mars soils. *Geochimica et Cosmochimica Acta*, **66**, 2801–2806.

Barrón, V., Torrent, J., and de Grave, E. (2003) Hydromaghemite, an intermediate in the hydrothermal transformation of 2-line ferrihidrite into hematite. *American Mineralogist*, **88**, 1679–1688.

Batlle, X. and Labarta, A. (2002) Finite-size effects in fine particles: magnetic and transport properties. *Journal of Physics D – Applied Physics*, **35**, R15–R42.

Bomatí-Miguel, O., Mazeina, L., Navrotsky, A., and Veintemillas-Verdaguer, S. (2008) Calorimetric study of maghemite nanoparticles synthesized by laser-induced pyrolysis. *Chemistry of Materials*, **20**, 591–598.

Brunauer, S., Emmett, P.H., and Teller, J. (1938) Adsorption of gases in multimolecular layers. *Journal of the American Chemical Society*, **60**, 309–319.

Chernyshova, I.V., Hochella Jr, M.F., and Madden, A.S. (2007) Size-dependent structural transformations of hematite nanoparticles. 1. Phase transition. *Physical Chemistry Chemical Physics*, **9**, 1736–1750.

Coffey, W.T., Crothers, D.S.F., Kalmykov, Yu.P., Massawe, E.S., and Waldron, J. T. (1993) Exact analytic formulae for the correlation times for single domain ferromagnetic particles. *Journal of Magnetism and Magnetic Materials*, **127**, L254–L260.

Cornell, R.M. and Schwertmann, U. (1979) Influence of organic anions on the crystallization of ferrihydrite. *Clays and Clay Minerals*, **33**, 219–227.

Cornell, R.M. and Schwertmann, U. (2003) *The Iron Oxides*. VCH, Weinheim, Germany, 573 pp.

Cullity, B.D. (1972) *Introduction to Magnetic Materials*, Addison-Wesley Publishing, Reading, Massachusetts, USA, 666 pp.

Duarte, E.L., Itri, R., Lima, E., Baptista, M.S., Berquó, T.S., and Goya, G.F. (2006) Large magnetic anisotropy in ferrihydrite nanoparticles synthesized from reverse micelles. *Nanotechnology*, **17**, 5549–5555.

Eggleton, R.A. and Fitzpatrick, R.W. (1988) New data and a revised structural model for ferrihydrite. *Clays and Clay Minerals*, **36**, 111–124.

Gálvez, N., Barrón, V., and Torrent, J. (1999) Effect of phosphate on the crystallization of hematite, goethite, and lepidocrocite from ferrihydrite. *Clays and Clay Minerals*, **47**, 304–311.

Glasauer, S.M., Friedl, J., and Schwertmann, U. (1999) Properties of goethites prepared under acidic and basic conditions in the presence of silicate. *Journal of Colloid and Interface Science*, **216**, 106– 115.

Guardia, P., Batlle-Brugal, B., Roca, A.G., Iglesias, O., Morales, M.P., Serna, C.J., Labarta, A., and Battle, X. (2007) Surfactant effects in magnetite nanoparticles of controlled size. *Journal of Magnetism and Magnetic Materials*, **316**, E756–E759.

Jambor, J.L. and Dutrizac, J.E. (1998) Occurrence and constitution of natural and synthetic ferrihydrite, a widespread iron oxyhydroxide. *Chemical Reviews*, **98**, 2549–2585.

Janney, D.E., Cowley, J.M., and Buseck, P.R. (2000) Structure of synthetic 2-line ferrihydrite by electron nanodiffraction. *American Mineralogist*, **85**, 1180–1187.

Janney, D.E., Cowley, J.M., and Buseck, P.R. (2001) Structure of synthetic 6-line ferrihydrite by electron nanodiffraction. *American Mineralogist*, **86**, 327–335.

Jansen, E., Kyek, A., Schäfer, W., and Schwertmann, U. (2002) The structure of six-line ferrihydrite. *Applied Physics A. Materials Science & Processing*, **A74**, A1004–S1006.

Lippens, B.C. and de Boer, J.H. (1965) Studies on pore systems in catalysts. V. The t method. *Journal of Catalysis*, **4**, 319–323.

Liu, Q.S., Barrón, V., Torrent, J., Eeckhout, S.G., and Deng, C.L. (2008) Magnetism of intermediate hydromaghemite in the transformation of 2-line ferrihydrite into hematite and its paleoenvironmental implications. *Journal of Geophysical Research – Solid Earth*, **113**, B01103, doi:10.1029/2007JB005207.

Manceau, A. and Gates, W.P. (1997) Surface structural model for ferrihydrite. *Clays and Clay Minerals*, **45**, 448–460.

McHale, J.M., Auroux, A., Perrotta, A.J., and Navrotsky, A. (1997) Surface energies and thermodynamic phase stability in nanocrystalline aluminas. *Science*, **277**, 788–791.

Michel, F.M., Ehm, L., Antao, S.M., Lee, P.L., Chupas, P.J., Liu, G., Strongin, D.R., Schoonen, M.A.A., Phillips, B.L., and Parise, J.B. (2007a) The structure of ferrihydrite, a nanocrystalline material. *Science*, **316**, 1726–1729.

Michel, F.M., Ehm, L., Liu, G., Han, W.Q., Antao, S.M., Chupas, P.J., Lee, P.L., Knorr, K., Euler, H., Kim, J., Grey, C.P., Celestian, A.J., Gillow, J., Schoonen, M.A.A., Strongin, D.R., and Parise, J.B. (2007b) Similarities in 2- and 6-line ferrihydrite based on pair distribution function analysis of X-ray total scattering. *Chemistry of Materials*, **19**, 1489–1496.

Morales, M.P., Veintemillas-Verdaguer, S., Montero, M.I., Serna, C.J., Roig, A., Casas, L., Martínez, B., and Sandiumenge, F. (1999) Surface and internal spin canting in gamma-Fe_2O_3 nanoparticles. *Chemistry of Materials*, **11**, 3058–3064.

Navrotsky, A., Mazeina, L., and Majzlan, J. (2008) Size-driven structural and thermodynamic complexity in iron oxides. *Science*, **319**, 1635–1638.

Reeves, N.J. and Mann, S. (1991) Influence of inorganic and organic additives on the tailored synthesis of iron oxides. *Journal of the Chemical Society – Faraday Transactions*, **87**, 3875–3880.

Schwertmann, U. (1985) Occurrence and formation of iron oxides in various pedoenvironments. Pp. 267–308 in: *Iron in Soils and Clay Minerals* (J.W. Stucki, B.A. Goodman and U. Schwertmann, editors). NATO ASI series No. 217, Dordrecht, The Netherlands.

Silva, N.J.O., Amaral, V.S., Carlos, L.D., Rodríguez-González, B., Liz-Marzán, L.M., Millán, A., Palacio, F., and Bermúdez, V. de Zea. (2006) Structural and magnetic studies in ferrihydrite nanoparticles formed within organic-inorganic hybrid matrices. *Journal of Applied Physics*, **100**, 054301–054307.

Torrent, J. and Guzmán, R. (1982) Crystallization of Fe (III)-oxides from ferrihydrite in salt solutions: osmotic and specific ion effects. *Clay Minerals*, **17**, 463–469.

Torrent, J., Guzmán, R., and Parra, M.A. (1982) Influence of relative-humidity on the crystallization of Fe(III) oxides from ferrihydrite. *Clays and Clay Minerals*, **30**, 337–340.

Torrent, J., Barrón, V., and Liu, Q. (2006) Magnetic enhancement is linked to and precedes hematite formation in aerobic soil. *Geophysical Research Letters*, **33**, L02401, doi:10.1029/2005GL024818.

Torrent, J., Liu, Q., Bloemendal, J., and Barrón, V. (2007) Magnetic enhancement and iron oxides in the upper Louchuan loess-paleosol sequence, Chinese Loess Plateau. *Soil Science Society of America Journal*, **71**, 1570–1578.

Vestal, C.R. and Zhang, Z.J. (2003) Effects of surface coordination chemistry on the magnetic properties of $MnFe_2O_4$ spinel ferrite nanoparticles. *Journal of the American Chemical Society*, **125**, 9828–9833.

Wilke, M., Farges, F., Petit, P.-E., Brown, Jr., G.E., and Martin, F. (2001) Oxidation state and coordination of Fe in minerals: An Fe K-XANES spectroscopic study. *American Mineralogist*, **86**, 714–730.

Zergenyi, R.S., Hirt, A.M., Zimmermann, S., Dobson, J.P., and Lowrie, W. (2000) Low-temperature magnetic behavior of ferrihydrite. *Journal of Geophysical Research – Solid Earth*, **105** 8297–8303.

Zhao, J., Huggins, F.E., Feng, Z., and Huffman, G.P. (1994) Ferrihydrite: surface structure and its effects on phase transformation. *Clays and Clay Minerals*, **42**, 737–746.

(*Received 2 November 2007; revised 24 September 2008; Ms. 0096; A.E. H. Stanjek*)